Modeling protein interaction network and mechanisms in exocytosis

Wen Zhou[1,*], Tian Xia[2,*], Jiansong Tong[3,*], Julie Dickerson[2,†], and Bo Su[1,†], Xun Gu[4,†]

[1]*Department of Mathematics, Iowa State University, Ames, IA 50010 , e-mail:* riczw@iastate.edu; bosu@iastate.edu

[2]*Program of Bioinformatics and computational biology, Iowa State University, Ames, IA 50010, e-mail:* netscape@iastate.edu; julied@iastate.edu

[3]*Department of Biochemistry, Biophysics, and Molecular Biology, Iowa State University, Ames, IA 50010, e-mail:* tjs100@iastate.edu

[4]*Department of Genetics, Development and Cell Biology , Iowa State University, Ames, IA 50010, e-mail:* xgu@iastate.edu

Abstract

Exocytosis is an essential process in all eukaryotic cells that allows communication in cells through vesicles which contain a wide range of intracellular molecules such as hormones, matrix proteins and neurotransmitters. Recent studies have shown this process is regulated by molecular interactions among a group of well defined and conserved proteins. To gain insight into the dynamics of these interactions, we use protein interaction network modeling to investigate exocytotic system (particularly in endocrine) computationally and mathematically . The protein interactions are formulated into ordinary differential equations (ODE). We then apply a novel mathematic approach to estimate model parameters from experimental data for SNAREs-only network (with three key proteins), which is a subset of this system. Our approach is able to sense temporal changes in protein concentration and ratios of multiple proteins and precisely reconstruct the dynamical process of exocytosis, including vesicle docking, priming and fusion. Additionally, the model suggests that initial concentration of synaptic proteins plays a crucial role in efficiency of vesicle fusion, based on system stability analysis.

Keywords: *SNARE proteins, exocytosis, fusion, mathematical modeling, protein interaction network, stability analysis*

1. Introduction

Exocytosis is the fundamental physiological process that leads the traffic of vesicles to bind to and fuse with the plasma membrane, thereby releasing its vesicle contents into targeted cells that control many cellular processes, including endocrine, exocrine and neurotransmission. It forms the underpinning mechanism of cell to cell communication in multicellular organisms by means of a wide range of extracellular signals. Efforts made by genetic, biochemical, structural, and functional studies to unravel exocytosis show that it occurs in multiple steps including vesicle trafficking, docking, priming and fusion [24] which are mediated by a series of protein interactions among cytoskeletal, secretory or synaptic vesicle, plasma membrane and cytosolic proteins. It is believed that by forming complexes, SNARE proteins occupy a central position in this process which consists of vesicular (v-)SNARE and target(t-) SNARE protein isoforms, like VAMP/synaptobrevin, SNAP-25 and syntaxin respectively [7, 12]. Additionally, members of the Sec1/Munc18 (SM) protein family are thought to improve the specificity of SNARE-mediated fusion through different modes of interactions [3, 6, 26]. For the Ca^{2+} triggers exocytosis, the protein family synaptotagmin serves as Ca^{2+} sensor for regulating exocytotic process [4, 5, 15]. Recent work also suggests that the protein, complexin, functions as a clamp to regulate SNAREs in a fusion-ready manner in response to sudden calcium influx trigger [10]. These studies are based on a variety of biological techniques which provide valuable insights into exocytosis mechanisms. However, much of the process remains unknown due to the complexity of system. Exocytosis has not been investigated from the biological system point of view. Ashery and his colleagues proposed a computational platform to model the exocytotic process [18] . They formulated these protein interactions into a sequential (feed forward only) interaction pathway, used ODE to describe the exocytotic system dynamics, and applied genetic algorithm to estimate model parameters.

In this paper, we present a framework for systemically modeling the exocytotic process, particularly the fusion process. As in Ashery's work, we interpret the dynamics and architecture of the complex system by constructing ODEs. In contrast to Ashery's work, our work takes feedback effect into account and can more realistically and ac-

∗ Equal contribution.
† corresponding authors.

curately model these interactions occurring among not only SNAREs but regulatory proteins as well. It is important to notice that the concentration of proteins, complexes keeps changing in both *vivo* and *vitro* environments. Hence, our model includes all of the proteins and complexes to make it self-contained. We use the techniques of inverse problem to identify the parameters for the model. Through the method, we are able to recover the parameters and optimize them based on limited supporting data. According to [2], SNAREs-only network carries the fundamental mechanism for fusion and exocytosis, we therefore mainly study the stability behavior of this system hereby. Experimental results based on the computational implementation of our framework show our model can precisely reconstruct biologically experimental observations, including different fusion efficiency caused by change of SNARE proteins' concentration and multiple intermediates in SNARE-induced membrane fusion. It also suggests by virtue of stability analysis that the initial concentrations of SNARE proteins play a crucial role in exocytotic vesicle fusion step with plasma membrane. The rest of this paper is organized as follows: we start with brief description of our protein interaction network mechanism in Section 2.1. In Section 2.2 we formulate the biological model into mathematical ODEs. Section 3 gives a brief introduction of the parameter identification and stability analysis (with numerical experimental results as well). We conclude our discussion in Section 4.

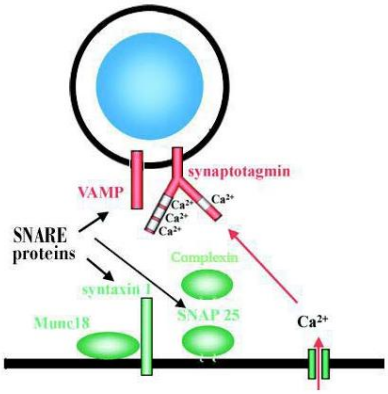

Fig 1. Panorama of protein interaction in complete fusion process.

2. Mathematical Modeling

2.1. Protein interaction and mechanism

The exocytotic process is a comprehensive combination of interacting events and independent reactions of well defined proteins (refer to figure 1); so is the fusion process, one of the most interesting and important part of exocytosis. Accordingly, the process is able to be transformed into a set of binary reactions, and suggested by [2, 13], most protein dynamics are homogeneous, which implies that the effect of random motion of protein molecules are sufficiently small to be negligible. We therefore set up the model based on an ODE system to describe the interaction of proteins and their intermediate complexes.

The essential elements considered for the mathematical model are: synaptosome-associated protein of 25 kDa (SNAP25), syntaxin, vesicle-associated membrane protein (VAMP2), MUNC18, complexin, synaptotagmin, and Ca^{2+} ions. The relationship connecting them is considered as a network, which is shown in the figure 3.

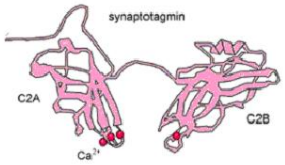

Fig 2. Structure of synaptotagmin. Clearly illustrate the tandem structure of synaptotagmin family.

The well known foundations [2, 7, 12] for this systematic processes are the reactions (2.1) and (2.2) as below

$$SNAP25 + syntaxin \underset{k_{-1}}{\overset{k_1}{\rightleftharpoons}} tSNARE \tag{2.1}$$

$$tsanre + VAMP2 \underset{k_{-2}}{\overset{k_2}{\rightleftharpoons}} FHC, \tag{2.2}$$

where FHC stands for four helical bundle, and it has been suggested that formation of this complex is the main factor to promote membrane fusion, which is the essential part of exocytosis. According to [10], function of complexin is summarized as (2.3) and (2.5), which reflects to its clamp function

$$FHC + complexin \underset{k_{-3}}{\overset{k_3}{\rightleftharpoons}} FC \tag{2.3}$$

where FC is a generic notation for the intermediate complex of FHC and complexin.

Ca^{2+} is the main or even the only trigger for the initiation of regulated exocytosis in intracellular case. Ca^{2+} are released from both external or internal stores [2, 4, 5, 15]. Suggested by [1, 2], the regulation of Ca^{2+} is executed through stimulating synaptotagmin; furthermore, the recruitment mechanism for Ca^{2+} are studied in [11] and it is known that Ca^{2+} ions bind the domain in a '1-3' process illustrated in the figure 2. A well known mechanism to characterize the regulatory function of synaptotagmin stimulated by Ca^{2+} is that it binds with SNARE complexes and stimulates the fusion (FHC) as suggested by [25].

Summarizing the above mechanism regarding Ca^{2+} and synaptotagmin, the reaction equations read

$$synaptotagmin + Ca^{2+} \underset{k_{-4}}{\overset{k_4}{\rightleftharpoons}} CaS \tag{2.4}$$

where CaS stands for the complex of synaptotagmin and one Ca^{2+} ion, and

$$CaS + 3Ca^{2+} + FC \underset{k_{-5}}{\overset{k_5}{\rightleftharpoons}} FHC^* + complexin \tag{2.5}$$

$$CaS + 3Ca^{2+} + tSNARE \underset{k_{-6}}{\overset{k_6}{\rightleftharpoons}} CT \tag{2.6}$$

$$CaS + 3Ca^{2+} + FHC \underset{k_{-7}}{\overset{k_7}{\rightleftharpoons}} FHC^* \tag{2.7}$$

where generic notation Tsc represents the intermediate complex of tSNARE and synaptotagmin binding four Ca2+ ions, and FHC* represents the complex of FHC and synaptotagmin binding four Ca2+ ions. It is noteworthy that reaction (2.4) is independent from the whole process.

MUNC18 is an important regulatory protein for the system. Current research [3, 6, 26] suggests that MUNC18 regulates the system through different modes. There are two significantly well accepted modes: 1) MUCNC 18 associates with syntaxin initially so that syntaxin is unavailable for assembly into the SNARE complexes at the beginning stage, and even later it can sequester the syntaxin (particularly, syntaxin I) from the other SNAREs; 2) MUNC18 stimulates the fusion process through associating with FHC. We therefore have the last two reaction mechanisms formulated as

$$MUNC18 + FHC \underset{k_{-8}}{\overset{k_8}{\rightleftharpoons}} FHC^{**} \tag{2.8}$$

where FHC** is the complex of MUNC18 and FHC, and it behaves likely to FHC to help the fusion process; and

$$MUNC18 + syntaxin \underset{k_{-0}}{\overset{k_0}{\rightleftharpoons}} Smc \tag{2.9}$$

where Smc is the generic name for the intermediate complex of MUNC18 and syntaxin.

Figure 3 summarizes the described reactions for fusion.

As a closure for the reaction system $(2.1) \sim (2.9)$, we remark that some results [20] suggest that self-association of syntaxin is possible such that

$$i \cdot syntaxin \underset{\epsilon_{-i}}{\overset{\epsilon_i}{\rightleftharpoons}} syntaxin_i \tag{2.10}$$

where $i = 5, 6, 7, 8$, syntaxin^i represents the complexes made of i syntaxins.

According to the reaction $(2.1) \sim (2.9)$, we develop a mathematical model using ordinary differential equations (ODE) that captures how the concentrations of different proteins and complexes vary along time and how they intersect with other species.

2.2. Mathematical modeling

Based on the law of mass action and Michaelis-Menten Kinetics, using conventional notation $[\cdot]$ to denote the concentration, the ODE system reads

$$\frac{d[SNAP25]}{dt} = -k_1[SNAP25][syntaxin] + k_{-1}[tSNARE] \tag{2.11}$$

$$\frac{d[syntaxin]}{dt} = -k_1[SNAP25][syntaxin] + k_{-0}[Smc] - k_0[syntaxin][MUNC18] + k_{-1}[tSNARE] \tag{2.12}$$

$$\frac{d[VAMP2]}{dt} = -k_2[tSNARE][VAMP2] + k_{-2}[FHC] \tag{2.13}$$

$$\frac{d[synaptotagmin]}{dt} = -k_4[synaptotagmin][Ca^{2+}] + k_{-4}[CaS] \tag{2.14}$$

$$\frac{d[complexin]}{dt} = -k_3[FHC][complexin] + k_5[CaS][FC][Ca^{2+}]^3 - k_{-5}[FHC^*][complexin] + k_{-3}[FC] \tag{2.15}$$

$$\frac{d[MUNC18]}{dt} = -k_0[MUNC18][syntaxin] + k_{-0}[Smc] + k_{-8}[FHC^{**}] - k_8[MUNC18][FHC] \tag{2.16}$$

$$\frac{d[FC]}{dt} = k_3[FHC][complexin] + k_{-5}[FHC^*][complexin] - k_{-3}[FC] - k_5[CaS][FC][Ca^{2+}]^3 \tag{2.17}$$

$$\frac{d[CT]}{dt} = k_6[CaS][tSNARE][Ca^{2+}]^3 - k_{-6}[CT] \tag{2.18}$$

$$\frac{d[CaS]}{dt} = k_{-6}[CT] + k_{-7}[FHC^*] - k_7[CaS][FHC][Ca^{2+}]^3 + k_{-5}[FHC^*][complexin] - k_5[CaS][FC][Ca^{2+}]^3 - k_6[CaS][tSNARE][Ca^{2+}]^3 - k_{-4}[CaS] + k_4[synaptotagmin][Ca^{2+}] \tag{2.19}$$

$$\frac{d[Smc]}{dt} = k_0[MUNC18][syntaxin] - k_{-0}[Smc] \tag{2.20}$$

$$\frac{d[tSNARE]}{dt} = k_1[SNAP25][sytaxin] + k_{-2}[FHC] + k_{-6}[CT] - k_{-1}[tSNARE] - k_2[tSNARE][VAMP2] - k_6[CaS][tSNARE][Ca^{2+}]^3 \tag{2.21}$$

$$\frac{d[FHC]}{dt} = k_2[tSNARE][VAMP2] + k_{-3}[FC] + k_{-8}[FHC^{**}] + k_{-7}[FHC^*] - k_{-2}[FHC] - k_3[FHC][complexin] - k_8[MUNC18][FHC] - k_7[CaS][FHC][Ca^{2+}]^3 \tag{2.22}$$

$$\frac{d[FHC^*]}{dt} = k_5[CaS][FC][Ca^{2+}]^3 + k_7[CaS][FHC][Ca^{2+}]^3 - k_{-5}[FHC^*][complexin] - k_{-7}[FHC^*] \tag{2.23}$$

$$\frac{d[FHC^{**}]}{dt} = k_8[MUNC18][FHC] - k_{-8}[FHC^{**}]. \tag{2.24}$$

The dynamics for Ca^{2+} in exocytosis is complex. To allow to exploring this model, we assume that during the fusion process, concentration of Ca^{2+} ions at active zone is

temporal dependent [8]. Therefore, the dynamics of Ca^{2+} ions around the region of fusion (active zone) are characterized as

$$\begin{aligned}\frac{d[Ca^{2+}]}{dt} =& k_{-6}[CT] + k_{-7}[FHC^*] + k_{-5}[FHC^*][complexin] \\ &- k_5[CaS][FC][Ca^{2+}]^3 - k_4[synaptotagmin][Ca^{2+}] \\ &- k_6[CaS][tSNARE][Ca^{2+}]^3 + k_{-4}[CaS] \\ &- k_7[CaS][FHC][Ca^{2+}]^3 + S(Ca^{2+}),\end{aligned} \tag{2.25}$$

where $S(Ca^{2+})$ is the recruitment source of calcium. For the *in vivo* case, concentration of Ca^{2+} ions stays on a constant level locally as both the external and internal sources keep the balance of Ca^{2+}, therefore (2.25) can be replaced by

$$Ca^{2+} = Constant. \tag{2.26}$$

Alternatively, if we include the effect of self-association (2.10), the system has changes for the equation about syntaxin

$$\begin{aligned}\frac{d[syntaxin]}{dt} =& -k_1[SNAP25][syntaxin] + k_{-0}[Smc] \\ &+ k_{-1}[tSNARE] - k_0[syntaxin][MUNC18] \\ &- \sum_{i=5}^{8} \epsilon_i [syntaxin]^i + \sum_{i=5}^{8} \epsilon_{-i}[syntaxin_i]\end{aligned} \tag{2.27}$$

and the system have other four supplementary equations describing the dynamics of self-associated complexes:

$$\frac{d[syntaxin_i]}{dt} = \epsilon_i [syntaxin]^i - \epsilon_{-i}[syntaxin_i] \tag{2.28}$$

where $i = 5, 6, 7, 8$.

Straightforward algebra shows this ODE system (2.11) $\sim$ (2.25)/(2.26) complies with the detailed balance principle and conservation of mass. For instance, the only products of the reactions involving MUNC18 are Smc and FHC**, thus the change of concentration of MUNC18 are only relevant to the concentration of that two complexes. We therefore investigate the subsystem involving MUNC18, Smc and FHC**

$$\begin{aligned}&\frac{d}{dt}\Big([Smc] + [MUNC18] + [FHC^{**}]\Big) = 0 \\ \Rightarrow &[MUNC18](t) = [MUNC18](0) - [Smc](t) - [FHC^{**}](t)\end{aligned} \tag{2.29}$$

since there are no Smc and FHC** initially, and it is consistent with the biological principle.

Denote all of the variables (concentrations) in (2.11) $\sim$ (2.25)/(2.26) by a vector U so that the ODE system is rewritten in a compact way

$$\frac{dU}{dt} = f(U) \tag{2.30}$$

where f is vector of functions on the right hand side of each equations. Some complexes are large enough so that to be more precise, we ought to consider their diffusion effect, so that system (2.31) is modified as

$$\frac{dU}{dt} = f(U) + D_U \cdot \Delta U \tag{2.31}$$

where D_U stands for the vector of diffusion coefficients of proteins, complexes and ions. Study of reaction diffusion equations (2.32) would be more interesting for some specific cases (in our unpublished work [31]).

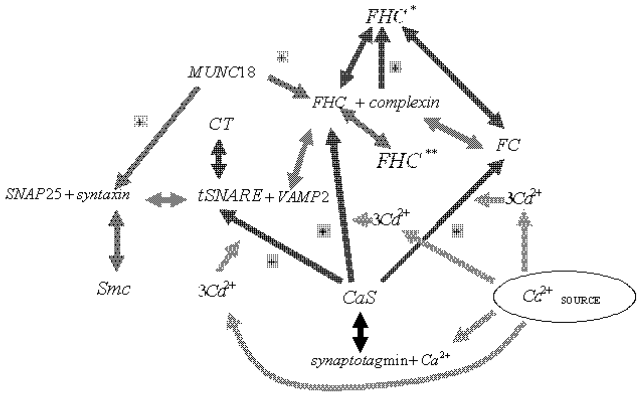

Fig 3. The whole process of fusion used in the mathematical model is shown. One direction arrows and symbol of " + " represent the reaction between proteins, ions and complexes, while full direction arrows connect two parts of a single reaction. It is noticeable that, topologically, the whole process is a combination of three interacting linear streams, instead of a single linear stream.

3. Parameter identification and stability analysis

3.1. Parameter recovery

To compare the ODE model with experimental results, and understand the nature of the process of fusion, it is crucial to have accurate parameter estimated. Among different methods of parameter identification, the technique of inverse problem takes advantage on two issues: the quantity of data it requires is small, and it guarantees the uniqueness and efficiency [14].

As well known and widely accepted machineries, reactions (2.1) and (2.2):

$$SNAP25 + syntaxin \underset{k_{-1}}{\overset{k_1}{\rightleftharpoons}} tSNARE + VAMP2 \underset{k_{-2}}{\overset{k_2}{\rightleftharpoons}} FHC$$

are fundamental for membrane fusion, and understanding them helps studying the quantitative nature of fusion and supports insight on the exocytosis with respect

to SNARE proteins. Therefore, in this present work, we mainly study the behavior of a subsystem involving only proteins SNAP25, syntaxin and VAMP2, which reads

$$\begin{aligned}
\frac{d[SNAP25]}{dt} &= -k_1[SNAP25][syntaxin] + k_{-1}[tSNARE] \\
\frac{d[syntaxin]}{dt} &= -k_1[SNAP25][syntaxin] + k_{-1}[tSNARE] \\
\frac{d[VAMP2]}{dt} &= -k_2[tSNARE][VAMP2] + k_{-2}[FHC] \\
\frac{d[tSNARE]}{dt} &= k_1[SNAP25][sytaxin] + k_{-2}[FHC] \\
&\quad - k_{-1}[tSNARE] - k_2[tSNARE][VAMP2] \\
\frac{d[FHC]}{dt} &= k_2[tSNARE][VAMP2] - k_{-2}[FHC].
\end{aligned} \tag{3.1}$$

and the framework of parameter identification is set based on (3.1).

There are two categories of unknown parameters in the ODE system, one is the initial concentration of different types of proteins and another is the reaction rate. According to the experimental data [17], we set the initial condition for system (3.1) to be:

$$\begin{aligned}
&[SNAP25](0) = [syntaxin](0) = 9[VAMP2](0) = 9\mu m/L \\
&[tsanre](0) = [FHC](0) = 0,
\end{aligned}$$

where symbol $[u](0)$ means the concentration of u at time $t = 0$.

To measure the fusion process, one uses fluorescence intensity in the experiments. To connect the concentration of core complex (FHC, FHC*, FHC**) to the fluorescence intensity, we assumes there exists an operator mapping the concentration of FHC (FHC*, FHC**) onto the space of fluorescence intensity $x(t)$, i.e. $x(t) = C([FHC], [FHC^*], [FHC^{**}])$ where C is assumed to be a linear operator according to [19]:

$$x(t) = c_1 \cdot [FHC^*] + c_2 \cdot [FHC^{**}] + c_3 \cdot [FHC] \tag{3.2}$$

where $c_i, (i = 1, 2, 3)$ are unknown constants and belong to some affective interval (alternatively, c is probably a nonlinear operator with respect to initial intensity, concentration and time such as $c = c(x(0), t, [FHC])$).

Based on the (3.2), we assume that the generated intensity of fluorescence due to fusion is

$$x_g(t) = [FHC](t) \cdot c \tag{3.3}$$

and the measured intensity of fluorescence is

$$x(t) = x_g(t) + x_0(t) \tag{3.4}$$

where $x_0(t)$ is a constant supply for fluorescence. By (3.4), we note that

$$\frac{dx}{dt} = \frac{dx_g}{dt} = c \cdot \frac{d[FHC]}{dt}. \tag{3.5}$$

Employing (3.3) and (3.5) in the system (3.1), denote

$$\begin{aligned}
&[SNAP25] = u_1, [syntaxin] = u_2, [VAMP2] = u_3, \\
&[tSNARE] = v_1, [FHC] = v_2 \ (x(t) = c \cdot v_2(t))
\end{aligned} \tag{3.6}$$

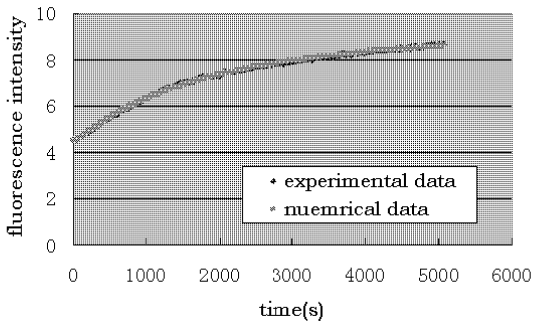

Fig 4. Comparison of numerical results with experimental data from [17]. The error is about 10^{-4}.

the new system reads

$$\begin{aligned}
\frac{du_1}{dt} &= -k_1 u_1 u_2 + k_{-1} v_1 \\
\frac{du_2}{dt} &= -k_1 u_1 u_2 + k_{-1} v_1 \\
\frac{du_3}{dt} &= -k_2 v_1 u_3 + k_c' x \\
\frac{dv_1}{dt} &= k_1 u_1 u_2 + k_c' x - k_{-1} v_1 - k_2 u_3 v_1 \\
\frac{dx}{dt} &= k_c v_1 u_3 - k_{-2} x
\end{aligned} \tag{3.7}$$

where $k_c = k_2 \cdot c$ and $k_c' = \dfrac{k_{-2}}{c}$. Thus, parameter recovery for the reactions (2.1) and (2.2) is equivalent to identify the parameters $(k_{\pm 1}, k_{\pm 2}, c)$ of system (3.7).

To recover the appropriate reaction rates, we apply technique introduced by [16, 27, 31] to (3.7). Some useful theorems are presented below and their proofs are left to [31].

Lemma 3.1. *The parameter identification of* (3.7) *is equivalent to the optimization problem of*

$$\begin{aligned}
p_\alpha &= arg \min_{U \in C[0,T), p \in \mathcal{P}} J(p) \\
&\text{subject to } \begin{cases} A(p)U = 0 \\ U(0) = U_0 \end{cases}
\end{aligned} \tag{3.8}$$

where $A(p)U = 0$ is the ODE system (3.7)*, U_0 is the initial conditions, $p = (k_{\pm 1}, k_{\pm 2}, c)$, $\mathcal{P}$ is the parameter space in R_+^5 and $J(p)$ is regularized energy functional*

$$J(p) = \frac{M}{2}||QU_p - U_e||^2 + \alpha||p||^2 + e^{||-p||^2} \tag{3.9}$$

where M and α are Tikhonov regularization parameter [14], Q is parameter-data mapping, U_e is experimental data, and $e^{||-p||^2}$ is the penalty function to guarantee the positivity of reaction rates [16].

Theorem 3.2. *Suppose the solution of* (3.7) $U = (u_1, u_2, u_3, v_1, x)$ *is smooth, where* $[0, T)$ *is the observation time, given observed data on each time point in* $[0, T)$*, the*

parameters identified by the inverse problem (3.8), (3.9) *are locally unique with respect to the initial condition.*

Taking advantage of the assumption that all of the reaction rates are constant (or at least in some intervals), the optimization problem (3.8) is solved through a gradient based method, which is discussed in details in [16]. The brief algorithm is sketched below:

Algorithm 3.3. ([16])
1. Given initial condition U_0, solving ODE system (3.1) by fourth order RK and mapping it on the observation data set,
2. Gradient representation: using forward difference to approximate ∇J,
3. Applying steepest descent to approach the global minimum starting with some initial guess,
4. Using adjoint scheme to approximate Hessian $\nabla^2 J$ of J,
5. Using the approximate solution given by step 2 as initial guess , and using Quasi-Newton method with $\nabla^2 J$ to find the appropriate parameter.

Using the data from [17], the identified parameters are shown in the table 1. We compare the numerical results based on the identified parameters with experimental data in figure 4, and the error is $\sim 10^{-4}$.

3.2. Stability analysis

Considering the subsystem (3.7) with v_2 instead of $x(t)$, the following analysis implies without regulatory, the final steady state, which is the final level of the fusion, is completely dependent on the initial concentration of proteins SNAP25, syntaxin, and VAMP2. Biologically, we conclude: first, the system depends only on the initial concentration of proteins; second, the system is very sensitive and rapidly reacts to the environment.

Define

$$c_1 = u_1(0) - u_2(0), c_2 = u_3(0), c_3 = u_1(0) \tag{3.10}$$

and,

$$K = \frac{k_{-1}}{k_1}, p = \frac{k_2}{k_1}, q = \frac{k_{-2}}{k_1}, \tag{3.11}$$

recalling (3.6) we have conclusion as the lemma following:

Lemma 3.4. *Based on the reaction rates recovered from experimental data and the references, assume the initial concentration of SNAP25 and syntaxin are same such that $c_1 = 0$, denote $K = \frac{k_{-1}}{k_1}$, provided $k_{-2} << k_2$, there are two stable steady states:*
if $c_2 > c_3$,

$$(0, 0, c_2 - c_3, 0, c_3); \tag{3.12}$$

otherwise

$$\Big(\frac{1}{2}\big[-K + \sqrt{K^2 - 4K(c_2 - c_3)}\big], \frac{1}{2}\big[-K + \sqrt{K^2 - 4K(c_2 - c_3)}\big], 0, c_3 - c_2 - \frac{1}{2}\big[-K + \sqrt{K^2 - 4K(c_2 - c_3)}\big], c_2\Big). \tag{3.13}$$

If $c_2 = c_3$, the steady state degenerates to $(0, 0, 0, 0, c_3)$, which is stable.

More interesting, without the assumption of same initial concentration of SNAP25 and syntaxin, stability analysis of system implies:

Theorem 3.5. *Based on the reaction rates recovered from experimental data and the references, provided $k_{-i} << k_i$ where $i = 1, 2$, there are four steady states:*
(i) if $c_1 \le 0$ and $c_3 \ge c_2$, the steady state is $(0, -c_1, 0, c_3 - c_2, c_2)$ and it is stable locally;
(i) if $c_1 \le 0$ and $c_3 \le c_2$, the steady state is $(0, -c_1, c_2 - c_3, 0, c_3)$ and it is a stable node locally;
(i) if $c_1 \ge 0$ and $c_3 \ge c_2 + c_1$, the steady state is $(c_1, 0, 0, c_3 - c_2 - c_1, c_2)$ and it is stable locally;
(i) if $c_1 \ge 0$, $c_3 \le c_2 + c_1$, and $c_3 \ge c_1$ the steady state is $(c_1, 0, c_2 + c_1 - c_3, 0, c_3 - c_1)$ and it is a stable node locally.

For more general case, the reaction ratio $K := \frac{k_{-1}}{k_1}$ and concentrations of SNARE proteins and complexes are in the same order so that a more version for theorem 3.5 is

Theorem 3.6. *According to the experimental data given by fluorescence assays and measurement of single molecule, reaction ratios hold*

$$K := \frac{k_{-1}}{k_1} \in (10^{-8}M, 10^{-6}M)$$

and

$$K' := \frac{k_{-2}}{k_2} \sim 10^{-10}M.$$

The steady states are

$$\begin{aligned} &P_1 = (0, -c_1, c_2 - c_3, 0, c_3), \text{ if } c_1 \le 0 \text{ and } c_3 \le c_2 \\ &P_2 = (c_1, 0, c_2 + c_1 - c_3, 0, c_3 - c_1), \text{ if } c_1 \ge 0,\ c_3 \le c_2 + c_1, \\ &\text{and } c_3 \ge c_1 \end{aligned} \tag{3.14}$$

and if $c_3 \ge c_2$ and $c_3 \ge c_2 + c_1$

$$P_3 = (u^*, u^* - c_1, 0, c_3 - u^* - c_2, c_2) \tag{3.15}$$

where

$$u^* = \frac{1}{2}\Big[(c_1 - K) \pm \sqrt{(K - c_1)^2 - 4K(c_2 - c_3)}\Big]. \tag{3.16}$$

P_1, P_2 are locally stable nodes, and P_3 is stable locally. When K is small sufficiently comparing to the concentrations of SNARE proteins and complexes, P_3 evolves to

$$\begin{aligned} P_3' &= (0, -c_1, 0, c_3 - c_2, c_2) \\ P_3'' &= (c_1, 0, 0, c_3 - c_2 - c_1, c_2). \end{aligned} \tag{3.17}$$

Lemma 3.4, theorem 3.5 and theorem 3.6 imply many deep natures of the fusion process; while numerical experiments imply that the behaviors of fundamental system match the known facts in both *vitro* and *vivo* (refer to figure 3.8 and 4). We hereafter present an interesting result based on it, which matches the well known experimental facts:

Corollary 3.7. *For the fundamental system involving SNAP25, syntaxin and VAMP2, preformed assays take advantage over the sequential one: first, preincubation advances reaction rates; second, preincubation support more fusion than sequential assays.*

Remark 3.8. In *vivo*, tSNARE is already preformed in the plasmic membrane; and carried by vesicles, vSNARE

TABLE 1. reaction rates for fundamental system

reaction rates	reaction involving	numerical interval	reference
k_1	$SNAP25 + syntaxin \rightarrow tSNARE$	$4.4 \times 10^3 M^{-1}s^{-1} \sim 2.3 \times 10^6 M^{-1}s^{-1}$	$6 \times 10^3 M^{-1}s^{-1}$, [21]
k_{-1}	$SNAP25 + syntaxin \leftarrow tSNARE$	$3.7594 \times 10^{-6} s^{-1} \sim 0.005493 s^{-1}$	$0.01 s^{-1}$, [23]
k_2	$tSNARE + VAMP2 \rightarrow FHC$	$3.6 \times 10^4 M^{-1}s^{-1} \sim 3.1 \times 10^6 M^{-1}s^{-1}$	$1 \times 10^5 M^{-1}s^{-1}$, [9]
k_{-2}	$tSNARE + VAMP2 \leftarrow FHC$	$1.96383 \times 10^{-4} s^{-1} \sim 0.00169 s^{-1}$	$4.2 \times 10^{-4} s^{-1}$, [29]
c	fusion-concentration constant	$1.235137\ cd/(M/L) \sim 6.1993083\ cd/(M/L)$	

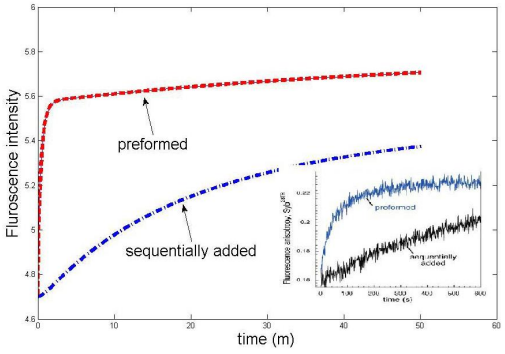

Fig 5. Comparison of numerical results and analysis with the experimental results: embedded plot is the experimental data from [23].

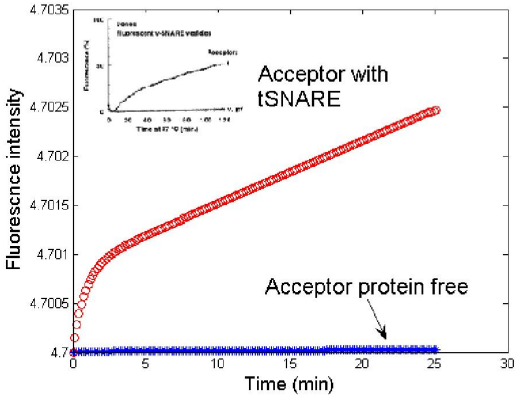

Fig 6. Donor vesicles containing the vSANRE VAMP, acceptor vesicles containing either no protein (protein free, no tSNARE) or preformed tSNAREs. Picture embedded in the plot is from [30].

(VAMP2 in our case) binds with it to generate fusion. Therefore, theorem 3.5 and 3.6 imply that the fundamental mechanism of fusion process is determined by the initial concentrations of tSNARE v_1 and vSNARE (VAMP2) u_3. The final fusion level depends on the one with smaller concentration among those SNARE proteins and complexes. In figure 6, we compare this theoretical results with numerical simulation and experimental fact.

Remark 3.9. Theorem 3.5, 3.6 and corollary 3.7 suggest that in *vivo*, there should not exist many free SNARE proteins such as SNAP25 and syntaxins, most of the SNARE proteins are already preincubation (preformed) into tSNAREs on the plasmic membrane.

4. Conclusion and discussion

In this study, we present a framework for modeling protein interaction network which are involved exocytotic process. The framework is based on classic chemical kinetic model that generates insights into system dynamics and stability. The computational experiments and mathematical analysis reveal that the frame reconstruct biological experimental observation successfully and is able to provide useful predictions.

References

[1] A. Bhalla, M.C. Chicka, W.C. Tucker and E.R. Chapman, "Ca^{2+} -synaptotagmin directly regulates t-SNARE function during reconstituted membrane fusion," nature structural and molecular biology, vol. 13, no. 4, pp. 323-330, 2006

[2] R. D. Burgoyne and A. Morgan, " Secretary Granule Exocytosis," Physiol. Rev., vol. 83, pp. 581-632, 2003

[3] R. D. Burgoyne and A. Morgan, "Membrane trafficking: three steps to fusion," Curr Biol, vol. 17, pp. 255-258, 2007.

[4] N. Brose, A. G. Petrenko, T. C. Sudhof, and R. Jahn, "Synaptotagmin: a calcium sensor on the synaptic vesicle surface," Science, vol. 256, pp. 1021-1025, 1992.

[5] E. R. Chapman, "Synaptotagmin: a Ca^{2+} sensor that triggers exocytosis?," Nat Rev Mol Cell Biol, vol. 3, pp. 498-508, 2002.

[6] L. F. Ciufo, J. W. Barclay, R. D. Burgoyne, and A. Morgan, "Munc18-1 regulates early and late stages of exocytosis via syntaxin-independent protein interactions," Mol Biol Cell, vol. 16, pp. 470-482, 2005.

[7] Y. A. Chen and R. H. Scheller, "SNARE-mediated membrane fusion," Nat Rev Mol Cell Biol, vol. 2, pp. 98-106, 2001.

[8] E. Dibenedetto, B. Su, "Homogenization in diffusion of

IP3," submitted
[9] D. Fasshauer and M. Margittai, "A transient N-terminal interaction of SNAP-25 and syntaxin nucleates SNARE assembly," J. Biol. Chem., vol. 279, pp. 7613-7621, 2004
[10] C. G. Giraudo, W. S. Eng, T. J. Melia, and J. E. Rothman, "A clamping mechanism involved in SNARE-dependent exocytosis," Science, vol. 313, pp. 676-80, 2006.
[11] C. Heinemann, L.V. Ruden, R.H. Chow, and E. Neher, "A two-step model of secretion control in neuroendocrine cells," Pflügers Arch, vol. 424, pp. 105-112, 1993
[12] R. Jahn, T. Lang, and T. C. Sudhof, "Membrane fusion," Cell, vol. 112, pp. 519-33, 2003.
[13] J. Keener and J. Sneyd, Mathematical Physiology, New YorkL Springer-Verlag, 2001
[14] A. Lorenzi, An introduction to identification problems via functional analysis, Utrecht: VSP-BV, 2001
[15] R. C. Lin and R. H. Scheller, "Mechanisms of synaptic vesicle exocytosis," Annu Rev Cell Dev Biol, vol. 16, pp. 19-49, 2000.
[16] Y.J. Liu, P. Sacks, B. Su, W. Zhou, " Parameter identification and numerical simulation of chemotaxis process," submitted
[17] X.B.Lu, F. Zhang, J.A. McNew, Y.K. Shin, "Membrane fusion induced by neuronal SNAREs transits through hemifusion," J. Biol. Chem., vol. 280, No. 34, pp. 30538-30541, 2005
[18] A. Mezer, E. Nachliel, M. Gutman, and U. Ashery, "A new platform to study the molecular mechanisms of exocytosis," J Neurosci, vol. 24, pp. 8838-46, 2004.
[19] T. Moser, E. Neher, "Estimation of mean exocytic vesicle capacitance in mose adrenal chromaffin cells," Proc Natl Acad Sci USA, vol. 94, pp. 6735-6740, 1997
[20] K.M.S. Misura, R.H. Schelle, and W.I. Weis, "Self-association of the h3 region of syntaxin 1a implications for intermediates in snare complex assembly," J. Biol. Chem., vol. 276, No. 16, pp. 13273-13282, 2001
[21] M. Margittai, J. Widengren, E. Schweinberger, G.F. Schroder, S. Felekyan, E. Haustein, M. Konig, D. Fasshauer, H. Grubmuller, R. Jahn, C.A. Seidel, "Single-molecule fluroscence resonance energy transfer reveals a dynamic equilibrium between closed an dopen conformations of syntaxin I," Proc. Natl. Acad. Sci. U.S.A., vol. 100, pp. 15516-15521, 2003
[22] L. Perko, Differential equations and dynamical systems, New YorkL Springer-Verlag, 2000
[23] A.V. Pobbati, A. Stein, D. Fasshauer, "N- to C-terminal SNARE complex assembly promotes rapid membrane fusion," Science, vol.313, pp.673-676, 2006
[24] T. C. Sudhof, "The synaptic vesicle cycle," Annu Rev Neurosci, vol. 27, pp. 509-547, 2004.
[25] T. Sollner, M.K. Bennett, S.W. Whiteheart, R. Scheller, and J.A. Rothman, "Protein assembly-disassembly pathway in vitro that may correspond to sequential steps of synaptic vesicle docking, activatgion, and fusion," Cell, vol. 75, pp. 409-418, 1993
[26] J.S. Shen, D.C. Tareste, F.Paumet, J.E. Rothman, and T.J. Melia, "Selective activation of cognate SNAREpins by SEC1/MUNC18 proteins," Cell, vol. 128, pp. 183-195, 2007
[27] C.R. Vogel, Computational Methods for inverse problem, SIAM, 2002
[28] G. de Vries, T. Hillen, M. Lewis, J. Muller, B. Schonfisch, A course in mathematical biology-quantitative modeling with mathematical and computational methods, SIAM Philadelphia, 2006
[29] K. Weninger, M.E. Bowen, S. Chu, A.T.Brunger, "Singel-molecule studies of SNARE complex assembly reveal parallel and antiparallel configurations," Proc. Natl. Acad. Sci. U.S.A., vol. 100, pp.14800-14805, 2003
[30] T. Weber, B.V. Zemelman, J.A. McNew, B. Westermann, M. Gmachl, F.Parlati, T. H. Sollner, and J. E. Rothman "SNAREpins: Minimal Machinery for Membrane Fusion," Cell, Vol. 92, pp. 759-772,1998
[31] W. Zhou, T. Xian, J.S. Tong, J. Dickerson, Y.K. Shin , B.Su, and X. Gu, "Membrane fusion process with regulatory network," submitted
[32] W. Zhou, K. Dorman, D. Jones, and B. Su, "Mathematical modeling of immune respons in tissue," submitted